



This is a repository copy of *On the performance of an integrated communication and localization system: an analytical framework*.

White Rose Research Online URL for this paper:

<https://eprints.whiterose.ac.uk/208750/>

Version: Accepted Version

---

**Article:**

Gao, Y., Hu, H., Zhang, J. et al. (3 more authors) (2024) On the performance of an integrated communication and localization system: an analytical framework. IEEE Transactions on Vehicular Technology. ISSN 0018-9545

<https://doi.org/10.1109/TVT.2024.3364257>

---

© 2024 The Authors. Except as otherwise noted, this author-accepted version of a article published in IEEE Transactions on Vehicular Technology is made available via the University of Sheffield Research Publications and Copyright Policy under the terms of the Creative Commons Attribution 4.0 International License (CC-BY 4.0), which permits unrestricted use, distribution and reproduction in any medium, provided the original work is properly cited. To view a copy of this licence, visit <http://creativecommons.org/licenses/by/4.0/>

**Reuse**

This article is distributed under the terms of the Creative Commons Attribution (CC BY) licence. This licence allows you to distribute, remix, tweak, and build upon the work, even commercially, as long as you credit the authors for the original work. More information and the full terms of the licence here:

<https://creativecommons.org/licenses/>

**Takedown**

If you consider content in White Rose Research Online to be in breach of UK law, please notify us by emailing [eprints@whiterose.ac.uk](mailto:eprints@whiterose.ac.uk) including the URL of the record and the reason for the withdrawal request.



[eprints@whiterose.ac.uk](mailto:eprints@whiterose.ac.uk)  
<https://eprints.whiterose.ac.uk/>

# On the Performance of an Integrated Communication and Localization System: An Analytical Framework

Yuan Gao, Haonan Hu, Jiliang Zhang, *Senior Member, IEEE*, Yanliang Jin, Shugong Xu, *Fellow, IEEE* and Xiaoli Chu, *Senior Member, IEEE*

**Abstract**—Localization has become a prominent use case for 6G mobile networks, and the integrated localization and communication (ILAC) system represents an inevitable trend. To design and manage such ILAC systems effectively and efficiently, quantification of its performance bound, i.e., an analytical model that reveals the trade-off between communication and localization performance, is a crucial yet unresolved task. To address this, we proposed an analytical framework for an ILAC system that achieves communication and localization. Specifically, we derived a closed-form expression of the capacity loss versus localization Cramer-Rao lower bound (CRB) loss through time-domain and frequency-domain resource allocation. Through simulations, we validated our analytical model and observed that frequency-domain resource allocation is preferable in scenarios with fewer antennas at the next generation nodeB (gNB) and a larger distance between user equipment (UE) and gNB. Conversely, time-domain resource allocation is preferable in scenarios with more antennas and a smaller distance between UE and the gNB.

**Index Terms**—Integrated Communication and Localization, Resource Allocation, Performance Bound

## I. INTRODUCTION

Integrated sensing and communication (ISAC) that performs communication and sensing simultaneously by leveraging the same spectrum resource and hardware has been considered a key technology of 6G [1]. Sensing is expected to trigger various novel applications, such as smart cities, smart transportation systems and industrial Internet of Things (IoT). For the communication industries and operators, localization has been the most urgent and desirable sensing function, and has attracted wide attention [2], [3].

Resource allocation has been studied for integrated localization and communication (ILAC). The ILAC performance

This paper is supported in part by the Innovation Program of Shanghai Municipal Science and Technology Commission under Grant 22511103202, the Horizon Europe research and innovation program under grant 101086219, the UK EPSRC grant EP/X038971/1, and Guangdong Province Science and Technology Project 2023A0505050127.

Yuan Gao, Yanliang Jin and Shugong Xu are with the School of Communication and Information Engineering, Shanghai University, P.R.C, email: gaoyuansie@shu.edu.cn, jinyanliang@staff.shu.edu.cn and shugong@shu.edu.cn.

Haonan Hu. is with the School of Communication and Information Engineering, Chongqing University of Posts and Telecommunications, Chongqing, P.R.C, e-mail: huhn@cqupt.edu.cn.

Jiliang Zhang is with the College of Information Science and Engineering, Northeastern University, Shenyang, P.R.C, email: zhangjiliang1@mail.neu.edu.cn.

Xiaoli Chu is with the Department of Electronic and Electrical Engineering, The University of Sheffield, UK, e-mail: x.chu@sheffield.ac.uk.

trade-off was first investigated by allocating dedicated time-domain resources for communication and localization, respectively [4], [5]. On top of the time-domain resource sharing, the localization accuracy and data rate are further explored by optimizing the beam width for communication and localization, respectively [6]. A waveform optimization scheme was developed to maximize the mutual information of joint communication and localization [7], [8]. An optimal time-frequency-domain resource allocation algorithm is proposed to maximize the value of service of the ILAC system [9]. The performance tradeoff of various power-frequency-domain resource allocation scheme are revealed via simulation [10]. Joint time-frequency-spatial domain resource sharing enables a balance between data rate and localization error in [11], [12], while perfect CSI is assumed, which is impractical in real ILAC systems. In addition, all the above works are simulation-based and fail to reveal the performance bound quantitatively, resulting in providing quite limited insights for practical ILAC system [13]. Whereas an analytical framework that reveals the fundamental performance bound or trade-off between communication and localization for various resource allocation schemes is critical to designing and operating practical ILAC systems, which is not yet resolved.

To overcome the limitations of the existing research that are simulation-based, we are first to propose an analytical framework to quantify the performance bound of an ILAC system considering the channel estimation overhead and error, and reveal the performance trade-off between communication and localization. Our analytical framework is validated through simulation and provides great predictability for the system performance in time-domain and frequency-domain resource allocation. Using this analytical model, we further reveal the ILAC performance bound and the trade-off between communication and localization performance, which provide insights for practical ILAC system design and resource allocation.

## II. SYSTEM MODEL

As shown in Fig. 1, we consider an ILAC 5G NR system, where a 5G gNB equipped with a uniform linear array (ULA) of  $N_T$  antennas (antenna space of  $d_A$ ) transmits downlink communication signals to the user equipment (UE) and transmits positioning reference signal for localization.

Without loss of generality, the frame structure of the time-frequency resource in 5G is divided into communication and

TABLE I  
LIST OF ABBREVIATIONS.

Abbreviation	Description
$N_T$	Number of antennas equipped at the gNB
$d_A$	Antenna space at the gNB
$\tau_T$	Total number of symbols
$\tau_C$	Number of symbols for communication
$\tau_L$	Number of symbols for localization
$\tau_P$	Number of symbols for pilot
$B$	Total bandwidth of the spectrum resource
$B_C$	Bandwidth of the spectrum resource for communication
$B_L$	Bandwidth of the spectrum resource for localization
$(x_0, y_0)$	The localization of the gNB as an anchor
$(\hat{x}, \hat{y})$	The estimated localization of the UE
$\hat{\theta}, \hat{t}$	The estimated angle of arrival time of arrival of UE
$c$	The speed of light
$\gamma$	SNR
$\varsigma$	The coefficient dependent on the waveform
$\lambda$	The wavelength of the spectrum
$\beta$	The large-scale fading coefficient between UE and gNB
$\nu$	The mean square of the channel estimation
$\rho_{ul}, \rho_{dl}$	The nominal uplink and downlink
$P_{UE}, P_{gNB}$	The transmission power of the UE and gNB
$G_{gNB}, G_{UE}$	The power gain of the gNB and UE
$N$	The power of white noise

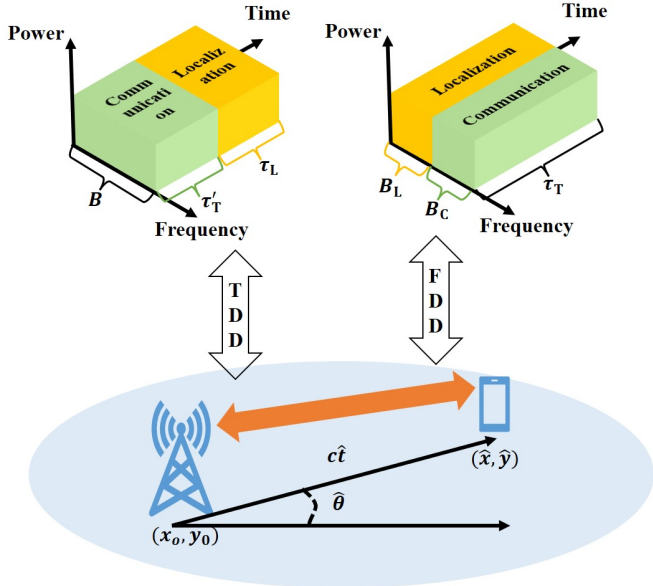


Fig. 1. System model of ILAC network, resource allocation in time- and frequency-domain

localization blocks for simplicity. The time-domain resource allocation for ILAC is illustrated in the top left of Fig. 1, where a total number of  $\tau_T$  symbols is divided into the communication block of  $\tau_C$  and the localization block with  $\tau_L$ . For the frequency-domain resource allocation in the top right of Fig. 1, the spectrum resource of total bandwidth of  $B$  is divided into the communication block of  $B_C$  and the localization block with  $B_L$ . The communication block consists of channel estimation consisting of  $\tau_P$  symbols and data transmission consisting of  $\tau_C - \tau_P$  symbols.

We consider this network to work in a downlink-only ILAC mode while uplink pilot is used for channel estimation.

Hence, the capacity of such network using maximum ratio is calculated as [14]:

$$C(B_C, \tau_C) = B_C \frac{\tau_C - \tau_P}{\tau_T} \ln \left( 1 + \frac{N_T \rho_{dl} \nu}{1 + \rho_{dl} \beta} \right), \quad (1)$$

where  $\beta$  is the large-scale fading coefficient and  $\nu = (\tau_P \rho_{ul} \beta^2) / (1 + \tau_P \rho_{ul} \beta)$  is the mean square of the channel estimation [14].  $\rho_{ul} = P_{UE} G_{gNB} G_{UE} / N$  and  $\rho_{dl} = P_{gNB} G_{gNB} G_{UE} / N$  are the nominal uplink and downlink signal to noise ratio (SNR), respectively.  $N$  is the white noise. This framework can be easily extended to the uplink-only ILAC mode or the time-division UL-DL ILAC mode by exploiting the uplink capacity also given in [14].

### III. ILAC

In the considered ILAC system in Fig. 1, each UE is served by the gNB that offers the largest received signal strength, while performing 2D-localization using the same gNB as an anchor with known location  $(x_0, y_0)$ . The estimated localization  $(\hat{x}, \hat{y})$  of the UE is calculated as:

$$\hat{x} = x_0 + \cos(\hat{\theta}) c \hat{t}, \quad (2a)$$

$$\hat{y} = y_0 + \sin(\hat{\theta}) c \hat{t}, \quad (2b)$$

where  $\hat{t}$  is the estimated time of arrival (ToA),  $\hat{\theta}$  is the angle of arrival (AoA),  $\theta$  is the angle between the UE and the orientation of the ULA, and  $c$  is the speed of light.

We adopt the widely-used Cramer-Rao lower bound (CRB) to measure the localization accuracy, which is mathematically the lowest estimation error for an estimation [15]. The localization CRB based on joint ToA and AoA estimation using Eq. (3) can be obtained using the chain rule given in [15]:

$$CRB_{\hat{x}} = c^2 t^2 \sin^2(\theta) CRB_{\hat{\theta}} + c^2 \cos^2(\theta) CRB_{\hat{t}}, \quad (3a)$$

$$CRB_{\hat{y}} = c^2 t^2 \cos^2(\theta) CRB_{\hat{\theta}} + c^2 \sin^2(\theta) CRB_{\hat{t}}, \quad (3b)$$

where  $CRB_{\hat{x}}$  and  $CRB_{\hat{y}}$  are the CRB of UE position in x-axis and y-axis of a 2-D plane, respectively.  $t$  and  $\theta$  are the real ToA and AoA of the UE, respectively.  $CRB_{\hat{\theta}}$  and  $CRB_{\hat{t}}$  are the CRB of ToA and AoA, respectively. The CRB of the UE localization estimation is further calculated as:

$$CRB_L = CRB_{\hat{x}} + CRB_{\hat{y}} = c^2 t^2 CRB_{\hat{\theta}} + c^2 CRB_{\hat{t}}, \quad (4)$$

where  $CRB_{\hat{\theta}}$  and  $CRB_{\hat{t}}$  are further given in [15], respectively, as:

$$CRB_{\hat{\theta}} = \frac{3\lambda^2}{4\pi^2 d_\lambda^2 \gamma \cos^2 \theta N_T (N_T - 1) (2N_T - 1) \tau_L}, \quad (5)$$

$$CRB_{\hat{t}} = \frac{3}{8\pi^2 B_L^2 (1 + \varsigma) \gamma N_T \tau_L}, \quad (6)$$

where  $\gamma$  is the SNR,  $\varsigma$  is the coefficient dependent on the waveform [15], and  $\lambda$  is the wavelength of the spectrum. As  $CRB_{\hat{\theta}}$  is relevant to  $\tau_L$ , whereas  $CRB_{\hat{t}}$  is relevant to  $\tau_L$  and  $B_L$ , Eq. (4) can be further denote as:

$$CRB_L(B_L, \tau_L) = c^2 t^2 CRB_{\hat{\theta}}(\tau_L) + c^2 CRB_{\hat{t}}(B_L, \tau_L). \quad (7)$$

Eq. (7) will be used for the following derivation and analysis of the ILAC performance.

### A. Time-Domain Resource Allocation

In the time-domain resource allocation ILAC illustrates in the top left of Fig. 1, we develop the following performance analysis framework.

**Definition 1.** The system capacity loss in time-domain is defined as the difference between the capacity achieved using all the time-domain resource, i.e.,  $\tau_T$ , and the capacity achieved using  $\tau_C$  symbols, which is calculated mathematically as:

$$\text{Loss}_C^t = C(B, \tau_T) - C(B, \tau_C). \quad (8)$$

**Definition 2.** The system localization CRB loss in time-domain is defined as the ratio between the the localization CRB achieved using  $\tau_L$  and the the localization CRB achieved using all the time-domain resource, i.e.,  $\tau_T$  symbols, which is calculated mathematically as:

$$L_L^t = \frac{CRB_L(B, \tau_L)}{CRB_L(B, \tau_T)} = \frac{\tau_T}{\tau_L}. \quad (9)$$

To be noted that  $\tau_C = \tau_T - \tau_L$ .

**Theorem 1.** In time domain resource allocation, the relationship between localization CRB loss  $L_L^t$  and capacity loss  $L_C^t$  is expressed as:

$$L_L^t = \frac{\tau_T}{\tau_T - \left( \frac{\tau_T}{\sqrt{\frac{N_T \Lambda \varepsilon}{\alpha}} + \sqrt{\frac{N_T \Lambda \varepsilon}{\alpha}} + \Lambda \tau_T \left( 2\sqrt{\frac{N_T \Lambda \varepsilon}{\alpha \tau_T}} + \Lambda - \frac{L_C^t}{B} \right)} \right)^2}, \quad (10)$$

where  $\Lambda = \ln(\alpha/(1+\delta))$ ,  $\alpha = 1 + (N_T + 1)\rho_{dl}\beta$ ,  $\varepsilon = \rho_{dl}/\rho_{ul}$  and  $\delta = \rho_{dl}\beta$ .

*Proof.* Proof of **Theorem 1** refers to Appendix A. ■

### B. Frequency-Domain Resource Allocation

In the frequency-domain resource allocation ILAC illustrates in the top right of Fig. 1, we develop the following performance analysis framework.

**Definition 3.** The system capacity loss in frequency-domain is defined as the difference between the capacity achieved using all the frequency-domain resource, i.e.,  $B$  bandwidth of spectrum, and the capacity achieved using  $B_C$  bandwidth of spectrum resource, which is calculated mathematically as:

$$L_C^f = C(B, \tau_T) - C(B_C, \tau_T). \quad (11)$$

**Definition 4.** The system localization CRB loss in frequency-domain is defined as the ratio between the the localization CRB achieved using  $B_L$  and the localization CRB achieved using all the frequency-domain resource, i.e.,  $B$  bandwidth of spectrum, which is calculated mathematically as:

$$L_L^f = \frac{CRB(B_L, \tau_T)}{CRB(B, \tau_T)}. \quad (12)$$

To be noted that  $B_C = B - B_L$ .

**Theorem 2.** In frequency domain resource allocation, the relationship between localization CRB loss  $L_L^f$  and capacity loss  $L_C^f$  is expressed as:

$$L_L^f = \frac{\frac{3t^2\lambda^2}{d_A^2 \cos^2\theta(N_T-1)(2N_T-1)} + \frac{12}{2B_L^2(1+\varsigma)}}{\frac{3t^2\lambda^2}{d_A^2 \cos^2\theta(N_T-1)(2N_T-1)} + \frac{12}{2B^2(1+\varsigma)}}, \quad (13)$$

where  $B_L$  is calculated as:

$$B_L = \frac{L_C^f \tau_T}{\tau_T \ln\left(\frac{\alpha}{1+\delta}\right) - 2\sqrt{\frac{\tau_T N_T \varepsilon \ln\left(\frac{\alpha}{1+\delta}\right) \varepsilon}{\alpha}} + \frac{N_T \varepsilon}{\alpha}}, \quad (14)$$

where  $\alpha = 1 + (N_T + 1)\rho_{dl}\beta$ ,  $\varepsilon = \rho_{dl}/\rho_{ul}$  and  $\delta = \rho_{dl}\beta$ .

*Proof.* Proof of **Theorem 2** refers to Appendix B. ■

## IV. SIMULATION RESULTS

### A. Simulation Settings

The ILAC system is operating on the 2.6 GHz spectrum with a maximum bandwidth of 20 MHz and a sub-carrier bandwidth of 180 KHz. The coherence time of this system contains 200 symbols. The minimum resource element of this system is 180 KHz  $\times$  1 symbol, which can be allocated for communication or localization.  $\zeta = 1$  is designed for optimal localization performance in the position reference signal. We consider the resource block for communication and localization to be continuous. Free-space path loss model is adopted to calculate the large-scale fading coefficient  $\beta$ . We consider a single-antenna UE and multiple-antenna omnidirectional gNB (implying that  $\theta = 0$ ) with antenna numbers of 8 and 32, and antenna space of  $d_A = \lambda/2$ . The antenna gain of gNB  $G_{gNB}$  and UE  $G_{UE}$  are calculated using the antenna beamforming gain in [12].  $P_{gNB} = 13\text{dBm}$ ,  $P_{gUE} = 13\text{dBm}$ . The white noise power density is  $-174\text{dBm/Hz}$ , resulting in  $N$  equals  $-101\text{dBm}$  for 20 MHz.

### B. Simulation Results Analysis

In Fig. 2, the trade-off between the capacity and the localization CRB in the time-domain and frequency-domain are demonstrated in scenario with 8 (Fig. 2(a)) and 32 antenna (Fig. 2(b)), respectively. The maximum capacity and minimum localization CRB are plotted in horizontal and vertical lines, respectively. The general insight is that the frequency-domain allocation outperforms the time-domain allocation in low SNR and/or smaller number of antennas scenarios, such as  $SNR = 10\text{dB}$  and  $20\text{dB}$  Fig. 2(a), and  $SNR = 10\text{dB}$  in Fig. 2(b). When increasing the antenna number, time-domain allocation tends to become effective, as demonstrated by comparing the  $SNR = 30\text{dB}$  results of Fig. 2(a) and Fig. 2(b). Time-domain allocation outperforms frequency-domain allocation in  $SNR = 30\text{dB}$  scenario in Fig. 2(b).

Due to the fundamental trade-off between capacity and localization CRB, it makes more sense to reveal the effectiveness of sacrificing capacity for localization gain, which is demonstrated in Fig. 3. A significant observation is that the capacity loss versus localization CRB loss achieved by time-domain resource allocation is much less affected by SNR than that achieved by frequency-domain resource allocation. Nevertheless, according to both Eq. (11) and Fig. 3, the capacity loss versus localization CRB loss achieved by frequency-domain resource allocation is much affectively by SNR. Specifically, a higher level gain of localization CRB can be achieved by sacrificing a certain level of capacity if SNR is smaller, i.e., larger distance between the gNB and UE. In addition, as indicated in Fig. 2, Fig. 3 also demonstrated that

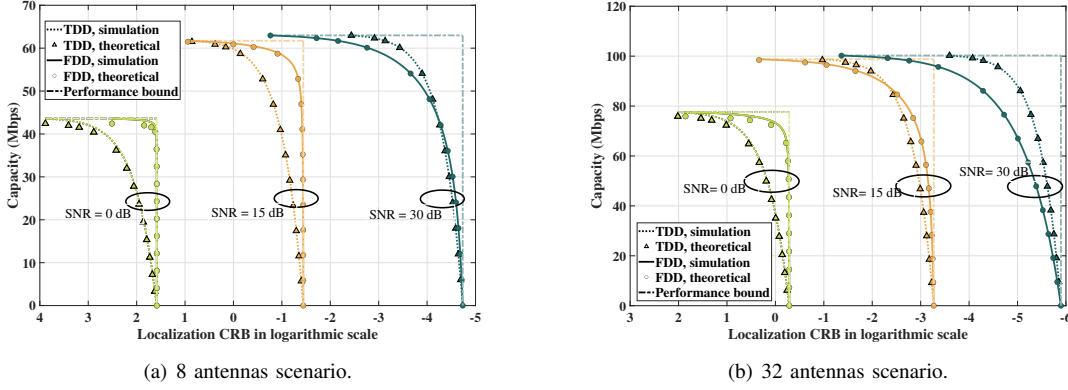


Fig. 2. Capacity versus CRB in frequency (solid line) and time (dotted line) domain. Time-domain and frequency-domain resource allocation are denoted as TDD and FDD, respectively.

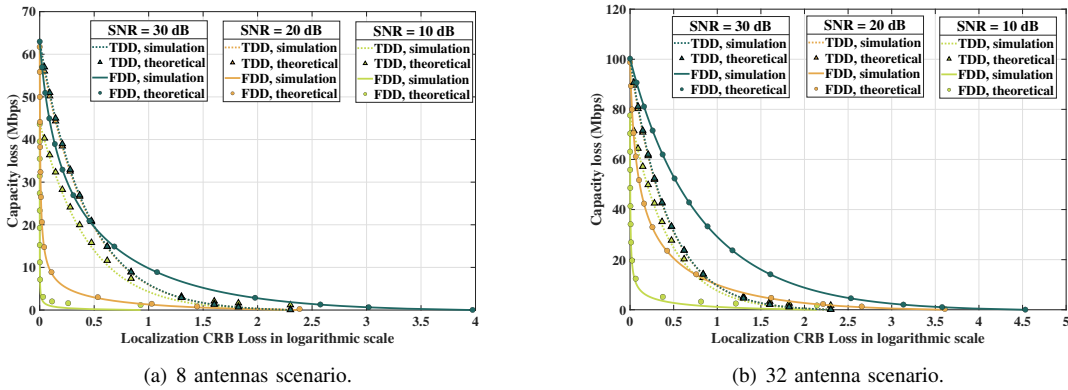


Fig. 3. Capacity loss versus CRB loss in frequency (solid line) and time (dotted line) domain. Time-domain and frequency-domain resource allocation are denoted as TDD and FDD, respectively.

the number of antennas affects significantly the effectiveness of time-domain and frequency-domain resource allocation to acquire localization CRB gain by sacrificing a certain level of capacity. With a smaller number of antennas, frequency-domain resource allocation outperforms time-domain resource allocation.

The above simulation results can provide further insights into achieving a better localization performance by choosing a resource allocation approach (time-domain or frequency-domain) concerning the number of antennas and SNR, i.e., distance between gNB and UE. In a nutshell, it is preferable to allocate frequency-domain resources for localization in scenarios with a smaller number of antennas and smaller SNR (larger distance between the gNB and UE), i.e., outdoor scenarios. While time-domain resource allocation is preferable in indoor scenarios with a larger number of antennas and larger SNR (smaller distance between the gNB and UE).

Another significant observation is the diminishing marginal utility of localization accuracy gain via capacity loss. This implies that sacrificing a slight level of capacity can obtain a fairly high level of localization accuracy, and a much lower level of localization accuracy gain is achieved by sacrificing the same level of capacity. Taking the simulation results in Fig. 2(a) SINR = 15 dB as an example, by using the frequency-domain resource allocation scheme, localization CRB of -1 dB

can be achieved by sacrificing around 5% of capacity (from around 62 to 59 Mbps), while localization CRB of -1.4 dB (slightly better than localization CRB of -1 dB) can only be achieved by sacrificing over 33% of capacity (from around 62 to 41 Mbps).

## V. CONCLUSION

In this article, we derived the closed-form performance bound of the communication and localization in an ILAC system. We also reveal the analytical relationship between the loss of capacity and the loss of localization CRB, and the fundamental effect of time-domain and frequency-domain resource allocation in terms of achieving the localization accuracy gain by sacrificing a certain level of capacity in various scenarios with different sizes. Such insights will provide guidance to exploit the radio resource more effectively to achieve communication and localization simultaneously in ILAC systems. We will extend our ILAC model into multiple-gNB and multiple-UE scenarios for a more comprehensive analysis.

## APPENDIX

### A. Proof of Theorem 1

*Proof.* To analytically analyse the capacity concerning the number of symbols  $\tau_P$  allocated for channel estimation, we

apply the inequality [16]:

$$\ln(1+x) \geq \ln(1+\bar{x}) + \frac{\bar{x}}{1+\bar{x}}(1-\frac{\bar{x}}{x}), \quad (15)$$

to transform Eq. (1) as:

$$C(B_C, \tau_C) \cong \frac{B_C}{\tau_T} \left( \tau_C \ln \left( \frac{\alpha}{1+\delta} \right) - \tau_C \frac{N_T \varepsilon}{\alpha \tau_P} - \tau_P \ln \left( \frac{\alpha}{1+\delta} \right) + \frac{N_T \varepsilon}{\alpha} \right), \quad (16)$$

where  $\alpha = 1 + (N_T + 1)\rho_{dl}\beta$ ,  $\varepsilon = \rho_{dl}/\rho_{ul}$  and  $\delta = \rho_{dl}\beta$ .

The optimal  $\tau_P$  that maximizes  $C$  can be easily calculated as:

$$\tilde{\tau}_P = \sqrt{\frac{\tau_C N_T \varepsilon}{\alpha \ln \left( \frac{\alpha}{1+\delta} \right)}}. \quad (17)$$

By substituting  $\tau_P$  with  $\tilde{\tau}_P$ , we have the optimal capacity  $C(B, \tau_C)$ , which is denoted as  $\tilde{C}(B, \tau_C)$ , calculated as:

$$\begin{aligned} \tilde{C}(B, \tau_C) &= \frac{B_C}{\tau_T} \left( \tau_C \ln \left( \frac{\alpha}{1+\delta} \right) - 2\sqrt{\frac{\tau_C N_T \ln \left( \frac{\alpha}{1+\delta} \right) \varepsilon}{\alpha}} + \frac{N_T \varepsilon}{\alpha} \right). \end{aligned} \quad (18)$$

For time domain resource allocation, the loss of capacity  $L_C^t$  is calculated as:

$$\begin{aligned} L_C^t &= \tilde{C}(B, \tau_T) - \tilde{C}(B, \tau_C) = \\ &= \frac{B}{\tau_T} \left( (\tau_T - \tau_C) \ln \left( \frac{\alpha}{1+\delta} \right) - 2(\sqrt{\tau_T} - \sqrt{\tau_C}) \sqrt{\frac{N_T \ln \left( \frac{\alpha}{1+\delta} \right) \varepsilon}{\alpha}} \right) \\ &\xrightarrow{a} -\tau_C \Lambda + 2\sqrt{\tau_C} \sqrt{\frac{N_T \Lambda \varepsilon}{\alpha}} - \tau_T \left( 2\sqrt{\frac{N_T \Lambda \varepsilon}{\alpha \tau_T}} - \Lambda + \frac{L_C^t}{B} \right) = 0, \end{aligned} \quad (19)$$

where transition (a) is achieved by defining  $\Lambda = \ln(\alpha/(1+\delta))$ . By solving Eq. (19) we have:

$$\tau_C = \left( \frac{\sqrt{\frac{N_T \Lambda \varepsilon}{\alpha}} + \sqrt{\frac{N_T \Lambda \varepsilon}{\alpha}} + \Lambda \tau_T \left( 2\sqrt{\frac{N_T \Lambda \varepsilon}{\alpha \tau_T}} - \Lambda + \frac{L_C^t}{B} \right)^2}{\Lambda} \right)^2 \quad (20)$$

By integrating Eq. (20) into the equality  $\tau_T = \tau_C + \tau_L$ , we obtain the expression of  $\tau_L$ . By further substituting  $\tau_L$  into Eq. (9), we have the capacity loss and localization CRB loss in Eq. (10). This closed the proof of **Theorem 1**. ■

### B. Proof of **Theorem 2**

*Proof.* For frequency domain resource allocation, by substituting Eq. (18) into Eq. (11), we obtain the loss of capacity  $L_C^f$  as:

$$\begin{aligned} L_C^f &= \tilde{C}(B, \tau_T) - \tilde{C}(B_C, \tau_T) = \\ &= \frac{B - B_C}{\tau_T} \left( \tau_T \ln \left( \frac{\alpha}{1+\delta} \right) - 2\sqrt{\frac{\tau_T N_T \ln \left( \frac{\alpha}{1+\delta} \right) \varepsilon}{\alpha}} + \frac{N_T}{\alpha} \right). \end{aligned} \quad (21)$$

By solving Eq. (19) we have:

$$B_L = \frac{L_C^f \tau_T}{\tau_T \ln \left( \frac{\alpha}{1+\delta} \right) - 2\sqrt{\frac{\tau_T N_T \ln \left( \frac{\alpha}{1+\delta} \right) \varepsilon}{\alpha}} + \frac{N_T}{\alpha}}. \quad (22)$$

By integrating Eq. (22) into Eq. (12), we have the capacity loss and localization CRB loss in Eq. (13). This closed the proof of **Theorem 2**. ■

### REFERENCES

- [1] J. A. Zhang, M. L. Rahman, K. Wu, X. Huang, Y. J. Guo, S. Chen, and J. Yuan, "Enabling joint communication and radar sensing in mobile networks—A survey," *IEEE Commun. Surv. Tutorials*, vol. 24, no. 1, pp. 306–345, 2021.
- [2] J. A. del Peral-Rosado, R. Raulefs, J. A. López-Salcedo, and G. Seco-Granados, "Survey of cellular mobile radio localization methods: From 1G to 5G," *IEEE Commun. Surv. Tutorials*, vol. 20, no. 2, pp. 1124–1148, 2017.
- [3] H. Wymeersch, A. Pärssinen, T. E. Abrudan, A. Wolfgang, K. Haneda, M. Sarajlic, M. E. Leinonen, M. F. Keskin, H. Chen, S. Lindberg *et al.*, "6G radio requirements to support integrated communication, localization, and sensing," in *2022 Joint European Conference on Networks and Communications & 6G Summit (EuCNC/6G Summit)*. IEEE, 2022, pp. 463–469.
- [4] D. Kumar, J. Saloranta, G. Destino, and A. Tölli, "On trade-off between 5G positioning and mmwave communication in a multi-user scenario," in *2018 8th International Conference on Localization and GNSS (ICL-GNSS)*. IEEE, 2018, pp. 1–5.
- [5] G. Destino and H. Wymeersch, "On the trade-off between positioning and data rate for mm-wave communication," in *IEEE International Conference on Communications Workshops (ICC Workshops)*. IEEE, 2017, pp. 797–802.
- [6] G. Ghatak, R. Koirala, A. De Domenico, B. Denis, D. Dardari, B. Uguen, and M. Coupechoux, "Beamwidth optimization and resource partitioning scheme for localization assisted mm-wave communication," *IEEE Trans. Commun.*, vol. 69, no. 2, pp. 1358–1374, 2020.
- [7] X. Yuan, Z. Feng, J. A. Zhang, W. Ni, R. P. Liu, Z. Wei, and C. Xu, "Spatio-temporal power optimization for MIMO joint communication and radio sensing systems with training overhead," *IEEE Trans. Veh. Technol.*, vol. 70, no. 1, pp. 514–528, 2020.
- [8] G. Kwon, A. Conti, H. Park, and M. Z. Win, "Joint communication and localization in millimeter wave networks," *IEEE J. Sel. Top. Signal Process.*, vol. 15, no. 6, pp. 1439–1454, 2021.
- [9] B. Li, X. Wang, Y. Xin, and E. Au, "Value of service maximization in integrated localization and communication system through joint resource allocation," *IEEE Transactions on Communications*, 2023.
- [10] F. Dong, F. Liu, Y. Cui, W. Wang, K. Han, and Z. Wang, "Sensing as a service in 6G perceptive networks: A unified framework for ISAC resource allocation," *IEEE Transactions on Wireless Communications*, 2022.
- [11] R. Koirala, B. Denis, B. Uguen, D. Dardari, and H. Wymeersch, "Localization and throughput trade-off in a multi-user multi-carrier mm-wave system," *IEEE Access*, vol. 7, pp. 167 099–167 112, 2019.
- [12] Y. Bao, B. Yu, B. Yin, X. Luo, and X. Lu, "Resource allocation for joint communication and localization systems with MU-MIMO," *IEEE Access*, vol. 10, pp. 124 649–124 662, 2022.
- [13] Z. Xiao and Y. Zeng, "An overview on integrated localization and communication towards 6G," *Science China Information Sciences*, vol. 65, pp. 1–46, 2022.
- [14] T. L. Marzetta, E. G. Larsson, and H. Yang, *Fundamentals of massive MIMO*. Cambridge University Press, 2016.
- [15] M. A. Richards, *Fundamentals of radar signal processing*. McGraw-Hill Education, 2014.
- [16] H. Yu, H. D. Tuan, T. Q. Duong, H. V. Poor, and Y. Fang, "Optimization for signal transmission and reception in a macrocell of heterogeneous uplinks and downlinks," *IEEE Transactions on Communications*, vol. 68, no. 11, pp. 7054–7067, 2020.